Int. J. Heat Mass Transfer. Vol. 34, No. 4/5, pp. 1219–1225, 1991
Printed in Great Britain

0017–9310/91 $3.00 + 0.00

Low Reynolds number simultaneously developing flows in the entrance region of parallel plates

T. V. NGUYEN
CSIRO Division of Mineral and Process Engineering, P.O. Box 312, Clayton, Victoria 3168, Australia

(*Received* 27 *February* 1990 *and in final form* 11 *June* 1990)

Abstract—The results of a numerical study of the simultaneously developing flow at low Reynolds number in the entrance region of a cascade of parallel horizontal plates with a uniform flow at upstream infinity are presented. The finite difference equations for the Navier–Stokes and energy partial differential equations, accounting for axial diffusion of momentum and heat, are solved by ADI and QUICK methods and the results extrapolated to zero mesh size with extended Richardson extrapolation. The isothermal flow results, incremental pressure drop and heat transfer numbers, and hydrodynamic and thermal entrance lengths are presented for $Pr = 0.7$ and Reynolds numbers between 1 and 20; and for constant wall temperature and constant wall heat flux boundary conditions. Accurate engineering correlations for the effects of the Re on various quantities are also obtained.

1. INTRODUCTION

AMONG the practical considerations that attract the continuing interest in the parallel plate passage geometry is that it offers high heat transfer rate and low pressure drop [1]. Two heat transfer boundary conditions are of primary interest—constant wall temperature, denoted here by subscript T, and constant wall heat flux, denoted by subscript H. For laminar fully developed flow, the parallel plate passage geometry has $Nu_T = 7.5407$, $Nu_H = 8.2353$ and $f\,Re = 24$ giving a higher $Nu/(f\,Re)$ than any other cross-sections [2]. Typical compact gas-to-gas heat exchangers have width/height ratios of at least 100 and require low Reynolds numbers and laminar flow.

The hydrodynamically developing flow between parallel plates has been solved by a variety of methods. Shah and London [2] presented values for K, the incremental pressure drop number, for large Reynolds numbers, and recommended a value of 0.674 for $K(\infty)$. This value is in excellent agreement with the correlating equation, $K(\infty) = 0.6779 + 4.5914/Re$ for $40 \leqslant Re \leqslant 2000$, given in ref. [3]. For the thermally developing flow, known as the Graetz–Nusselt problem, Shah [4] calculated the incremental heat transfer number N for developing flow and fully developed flow and obtained $N_T = 0.02348$ and $N_H = 0.0364$ with $Pe = \infty$. For the simultaneously developing flow problem, where both the velocity and temperature profiles are developing together, only a few solutions can be found in the literature. Hwang and Fan [5] obtained a numerical solution for the T and H boundary conditions with an assumed uniform flow at the entrance. Their Nusselt numbers are also reported in Shah and London [2].

This paper presents the results of a numerical study of the simultaneously developing flow, laminar flow, forced convection at Re ranging from 1 to 20 and $Pr = 0.7$ in the entrance region of a cascade of horizontal parallel plates. The flow is assumed to be uniform at upstream infinity. Two types of thermal boundary conditions are considered—a constant axial wall temperature and a constant and equal wall heat flux. In most previous numerical solutions, the approximations of various parameters, such as $K(\infty)$ and $N(\infty)$, deteriorate at the end of the hydrodynamic or thermal entrance. In the present work, discretization error is reduced by extrapolating three mesh sizes to zero mesh size giving accurate results and excellent agreement with previous solutions [3].

2. THE EQUATIONS AND THEIR SOLUTION

In Fig. 1 fluid is pictured as flowing through an array of horizontal parallel plates which are a centreline distance H apart. Both the temperature T_∞ and velocity U_∞ are uniform at upstream infinity. The plates are either kept at the same uniform temperature T_p or the heat flux is constant. The flow becomes fully developed far downstream. Dimensionless Cartesian coordinates are chosen such that the plate spacing is unity.

The equations of motion are written in terms of the stream function ψ and vorticity ζ, defined by

$$u = \frac{\partial \psi}{\partial y}, \quad v = -\frac{\partial \psi}{\partial x}, \quad \text{and} \quad \zeta = \frac{\partial v}{\partial x} - \frac{\partial u}{\partial y} \tag{1}$$

where u, v are velocity components in the x-, y-direction.

The dimensionless governing equations for vorticity, stream function and temperature, derived from the Navier–Stokes equations and subject to the usual Boussinesq approximations, are

NOMENCLATURE

D_h	hydraulic diameter
f	Fanning friction factor
Gr	Grashof number
H	channel width
K	incremental pressure drop number
$K(\infty)$	fully developed incremental pressure drop number
L_{hy}^+	hydrodynamic entrance length
L_{th}^*	thermal entrance length
n	number of interior mesh points
N	incremental heat transfer number
$N(\infty)$	fully developed incremental heat transfer number
Nu	Nusselt number
Δp	pressure drop
Pe	Péclet number
Pr	Prandtl number
Re	Reynolds number, $D_h U_\infty/\nu$
t	time
Δt	time step
T	temperature
T_p	plate temperature
T_∞	upstream temperature
u	dimensionless axial velocity
u_m	mean dimensionless axial velocity
U_∞	upstream velocity
v	dimensionless vertical velocity
x	dimensionless axial coordinate
x^+	dimensionless axial coordinate for the hydrodynamic problem, $x/(D_h\, Re)$
x^*	dimensionless axial coordinate for the thermal problem, $x/(D_h\, Re\, Pr)$
x_t	dimensionless transformed axial coordinate
y	dimensionless coordinate normal to the plates.

Greek symbols

α	thermal diffusivity
α_ϕ	false transient factor
ε	convergence factor
ζ	vorticity
θ	dimensionless temperature
ν	kinetic viscosity
ρ	fluid density
ψ	stream function.

Subscripts

bc	thermal boundary condition
fd	fully developed laminar flow
hy	hydrodynamic problem
H	constant heat flux boundary condition
m	mean
p	at the plate
t	transformed
th	thermal problem
T	constant temperature boundary condition
x	local
∞	free stream value.

$$\frac{\partial \zeta}{\partial t} = -u\frac{\partial \zeta}{\partial x} - v\frac{\partial \zeta}{\partial y} + \frac{1}{Re}\left(\frac{\partial^2 \zeta}{\partial x^2} + \frac{\partial^2 \zeta}{\partial y^2}\right) \quad (2)$$

$$0 = \left(\frac{\partial^2 \psi}{\partial x^2} + \frac{\partial^2 \psi}{\partial y^2}\right) + \zeta \quad (3)$$

$$\frac{\partial \theta}{\partial t} = -u\frac{\partial \theta}{\partial x} - v\frac{\partial \theta}{\partial y} + \frac{1}{Re\, Pr}\left(\frac{\partial^2 \theta}{\partial x^2} + \frac{\partial^2 \theta}{\partial y^2}\right) \quad (4)$$

in which $\theta = (T - T_\infty)/(T_p - T_\infty)$, $Re = U_\infty D_h/\nu$, and $Pr = \nu/\alpha$. Here H, ν, and α denote respectively the pitch of the plates, the kinetic viscosity and the thermal diffusivity.

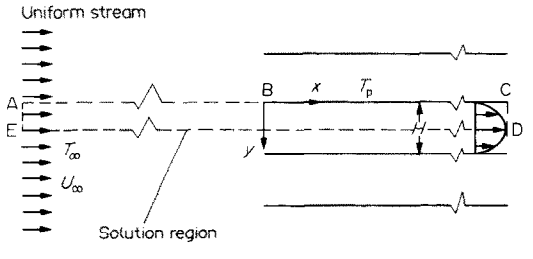

FIG. 1. Boundary conditions and solution region for parallel plate cascade.

Figure 1 shows the region ABCDE within which these equations were solved. The solution region is extended to infinity both upstream and downstream of the entry to the channels. Uniform flow was imposed on section AE: $u = 1$; $v = 0$; $\theta = 0$; $\zeta = 0$. Since the solution region represents the upper half of a channel formed by two parallel plates, the boundary conditions on sections AB and DE are: $v = 0$; $\partial u/\partial y = 0$; $\zeta = 0$. On section BC, the velocities are zero and the stream function is constant.

The coordinates and partial differential equations, equations (2)–(4), were transformed both upstream and downstream of the entrance using a function related to the downstream decay [6]. The transformed coordinate x_t is dimensionless and $-1 \leqslant x_t \leqslant 1$. It may be calculated from the dimensionless coordinate x in equations (2)–(4) using

$$x_t = \frac{(1 - \exp(-|x|/(0.089275 Re\, Pr)))x}{|x|}. \quad (5)$$

The transformed coordinates give a more equal

change in dependent variables over each grid element and points at upstream and downstream infinity. The number of grid elements required for a given discretization error is greatly reduced at the expense of slightly more computation per grid element.

Finite difference equations were derived from the transformed non-linear partial differential equations. Forward differences were used for the time derivatives and central differences for space derivatives. Quadratic upstream interpolation for convective kinematics (QUICK) [7] was used for the convective terms in both the momentum and energy equations to give stability with a discretization error of the order of the square of the mesh size.

The alternating direction implicit (ADI) iterative method was used to solve the non-linear finite difference equations simultaneously. Convergence was measured by calculating

$$\varepsilon_\phi = \frac{1}{n\phi_{\max}} \sum \frac{\phi^{n+1} - \phi^n}{\alpha_\phi \Delta t} \tag{6}$$

where n is the number of interior mesh points, $\phi_{\max}$ the maximum magnitude of ϕ, α_ϕ the false transient factor, and Δt the time step. Iteration was repeated until ε_ζ, ε_ψ, and ε_θ were all less than 10^{-9} so that the error in solving the finite difference equations was negligible and independent of grid size.

The dimensionless groups used in the present work are defined as follows (note that the standard coordinate $x^+ = x/(D_h\, Re)$ is used for the hydrodynamic problem and $x^* = x/(D_h\, Re\, Pr)$ for the thermal problem):

- the incremental pressure drop number

$$K(x) = \frac{\Delta p}{\rho u_m^2/2} - (f\, Re)_{fd}(4x^+); \tag{7}$$

- the local Nusselt number

$$Nu_x = 2\left(\frac{\partial \theta}{\partial y}\right)_{y=0} \Big/ (\theta_p - \theta_m) \tag{8}$$

where θ_m is the fluid bulk mean temperature;

- the mean Nusselt number

$$Nu_m = \frac{1}{x}\int_0^x Nu_x\, dx; \tag{9}$$

- the incremental heat transfer number

$$N_{bc}(x) = Nu_{m,bc}x^* - Nu_{bc}x^* \tag{10}$$

where subscript bc represents the associated thermal boundary conditions (T or H) and Nu_{bc} is the Nusselt number for fully developed flow.

Discretization error is the difference between the exact solution of the finite difference equations and the exact solution of the consistent partial differential equations. For the finite difference equations used here this is of the order of the grid size squared. It may be reduced to fourth order by extrapolation to zero grid size of the finite difference equation solutions for three different grid sizes. Each grid is solved with the same parameters and boundary conditions. The three grids chosen were 6×81, 11×161 and 21×321 mesh points in the y- and x-direction respectively, making each grid size half its predecessor. The following extrapolation formula was calculated from the general expression in Maclaine-cross [6]:

$$A = A3 - \frac{(A3 - A1) - 12(A3 - A2)}{21} \tag{11}$$

where $A3$ is the value at the smallest grid size, etc. It should be noted that the above formula is valid only for grids formed by successive mesh doubling, only for numerical methods which are uniformly second-order accurate, and for very tight iterative convergence. Other details of the solution method are discussed elsewhere [8].

3. ISOTHERMAL FLOW RESULTS

Equations (2)–(4) have been solved for the following Re: 1, 2, 5, 10, 15, and 20 and $Pr = 0.7$. It should be emphasized that Re is based on the hydraulic diameter $D_h = 2H$.

The extrapolated apparent Fanning friction factor–Reynolds number product $f_{app}\, Re$ is presented in Table 1 for the range of Re at each downstream location for the hydrodynamic entrance region of parallel plates. As can be seen here, $f_{app}\, Re$ is strongly dependent upon Re for low Re and has very steep gradients close to the entrance. Far downstream from the entrance, $f_{app}\, Re$ converges to the asymptotic fully developed value of 24.

For the hydrodynamic entrance length problem with a uniform flow far upstream, direct comparisons of $f_{app}\, Re$ for low Re flows are difficult as only a few solutions can be found in the literature. The only available correlation presented in Shah and London [2] gives values of $f_{app}\, Re$ which are independent of Re and much lower than those in Table 1. The computed apparent Fanning friction factor–Reynolds number product distributions are shown graphically in Fig. 2 for different Re. The dashed line representing the Shah and London correlation at $Re = \infty$ is also shown in the same figure.

The development of the centreline velocity for various Re is shown in Table 2 at each axial coarse mesh station for $Re = 1$, 2, 5, 10, 15, and 20. For these low Re flows with a uniform inlet condition at upstream infinity, the upstream diffusion of momentum is quite significant as can be seen from the centreline velocity at the entrance ($x^+ = 0$). The dimensionless velocity increases with decreasing Re at $x^+ = 0$ and is 24–33% higher than the mean velocity u_m. Inside the channel, wall shear takes effect and the centreline velocity increases with Re.

The fully developed incremental pressure drop number $K(\infty)$ is tabulated to four significant figures

Table 1. Apparent Fanning friction–Reynolds number product

	Re					
x^+	1	2	5	10	15	20
0.01282	181.9620	103.5631	58.6081	46.1770	43.0822	41.7367
0.02634	98.3552	61.1289	41.1411	35.7939	33.9890	33.0339
0.04063	70.8070	47.4956	35.4792	31.8083	30.5030	29.8591
0.05579	57.2620	40.9561	32.5395	29.6999	28.7353	28.2669
0.07192	49.3037	37.1669	30.6869	28.4210	27.6729	27.3097
0.08917	44.1220	34.6903	29.4107	27.5656	26.9624	26.6695
0.1077	40.5091	32.9254	28.4833	26.9522	26.4528	26.2103
0.1277	37.8586	31.5851	27.7811	26.4896	26.0685	25.8639
0.1495	35.8320	30.5199	27.2308	26.1273	25.7674	25.5926
0.1733	34.2260	29.6461	26.7865	25.8348	25.5243	25.3736
0.1996	32.9116	28.9127	26.4188	25.5927	25.3232	25.1924
0.2291	31.8038	28.2863	26.1079	25.3879	25.1531	25.0391
0.2625	30.8448	27.7429	25.8398	25.2114	25.0065	24.9069
0.3010	29.9945	27.2642	25.6042	25.0563	24.8776	24.7908
0.3466	29.2239	26.8349	25.3932	24.9174	24.7622	24.6868
0.4024	28.5098	26.4419	25.2000	24.7902	24.6565	24.5916
0.4743	27.8305	26.0716	25.0181	24.6704	24.5570	24.5019
0.5756	27.1574	25.7068	24.8388	24.5523	24.4589	24.4135
0.7489	26.4270	25.3120	24.6448	24.4246	24.3528	24.3179

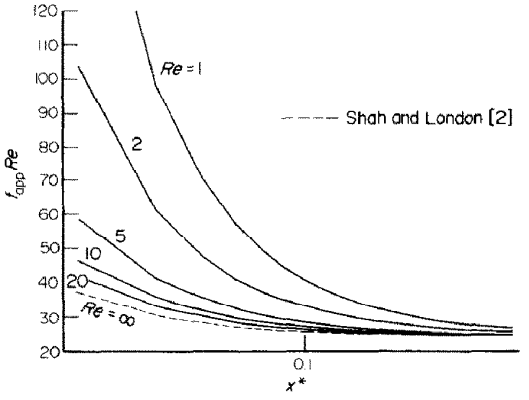

FIG. 2. Apparent Fanning friction factor–Reynolds number product for hydrodynamically developing flow.

in Table 3 for the range of Re and three mesh sizes. The three-point extrapolation to zero mesh size reduces but does not eliminate discretization error. A comparison of two-point and three-point extrapolations gives an indication of the magnitude of the remaining discretization error. Two-point extrapolation using the two smallest meshes gave values which are within 0.5% of the three-point extrapolation, see the last column in Table 3. It is believed that the residual discretization error in $K(\infty)$ is less than 0.5%.

For $1 \leqslant Re \leqslant 20$, $K(\infty)$ correlates very well with $1/Re$ and the following equation is given to approximate the values of $K(\infty)$ in Table 3 with the error ranging from 0.06% at $Re = 1$–1.1% at $Re = 20$

$$K(\infty) = 0.6090 + 6.6567/Re. \quad (12)$$

The fully developed incremental pressure drop number $K(\infty)$ can now be calculated for a wide range of Re from 1 to 2000 from the above equation and $K(\infty) = 0.6779 + 4.5914/Re$ given in ref. [3] with a maximum error of 1.1%. The values of $K(\infty)$ calculated from the correlation given by Chen [9], $K(\infty) = 0.64 + 38/Re$, also presented in Shah and London [2], are considerably higher for Re of up to

Table 2. u_{max}/u_m

	Re					
x^+	1	2	5	10	15	20
0.0	1.3340	1.3295	1.3149	1.2899	1.2657	1.2434
0.00633	1.3431	1.3477	1.3608	1.3813	1.3991	1.4137
0.01282	1.3522	1.3655	1.4014	1.4457	1.4711	1.4839
0.01949	1.3614	1.3827	1.4346	1.4802	1.4950	1.4988
0.02634	1.3704	1.3990	1.4594	1.4947	1.5000	1.5000
0.03338	1.3795	1.4143	1.4766	1.4995	1.5000	1.5000
0.04063	1.3884	1.4284	1.4877	1.5000	1.5000	1.5000
0.04809	1.3972	1.4411	1.4942	1.5000	1.5000	1.5000
0.05579	1.4058	1.4524	1.4978	1.5000	1.5000	1.5000
0.06372	1.4142	1.4623	1.4995	1.5000	1.5000	1.5000
0.07192	1.4224	1.4707	1.5000	1.5000	1.5000	1.5000
0.08917	1.4302	1.4778	1.5000	1.5000	1.5000	1.5000
0.10769	1.4379	1.4846	1.5000	1.5000	1.5000	1.5000

Table 3. Incremental pressure drop number $K(\infty)$

Re	6×81	11×161	21×321	Extrapolated	Difference (%)
1	6.3603	6.8860	7.1549	7.2707	0.36
2	3.5631	3.7832	3.8864	3.9300	0.23
5	1.9023	1.9236	1.9294	1.9314	0.00
10	1.3460	1.3055	1.2820	1.2718	0.18
15	1.1538	1.1030	1.0709	1.0566	0.34
20	1.0475	1.0045	0.9688	0.9521	0.50

Table 4. Hydrodynamic entrance length L_{hy}^+

Re	1	2	5	10	15	20
L_{hy}^+	0.18086	0.09172	0.03877	0.02142	0.01634	0.01323

600 and lower for Re above 1000 than those of the present study.

The hydrodynamic entrance length L_{hy}^+, defined as the duct length required to achieve a duct section maximum velocity of 99% of the fully developed value (1.5 for parallel plates), is presented in Table 4. $L_{hy}^+ = 0.011$ and is constant when based on a boundary layer type analysis [2]. However, when the complete set of Navier–Stokes equations is solved L_{hy}^+ is a strong function of Re for low Re flows, as seen in Table 4.

For $Pr = 0.7$ and $1 \leqslant Re \leqslant 20$, the following correlation is provided to approximate these values with the error ranging from 0.6% at $Re = 15$ to 3.5% at $Re = 2$:

$$L_{hy}^+ = 0.004004 + 0.1765/Re. \quad (13)$$

Chen [9] proposed an equation to calculate L_{hy}^+ for the hydrodynamically developing flow problem with a uniform flow at the entrance which gives values considerably higher than those in Table 4. The main contributing factor for this is the significant upstream diffusion of momentum in the case considered here, hence more developed velocity profiles and shorter entrance lengths.

4. CONSTANT WALL TEMPERATURE RESULTS

The fully developed Nusselt number for the constant wall temperature boundary condition is 7.5407 for the case of negligible axial heat conduction. However, when the effect of axial heat conduction in the fluid is included, the fully developed Nusselt number Nu_T is a strong function of the Péclet number for low Péclet number flows. The present numerical results are listed in Table 5. An additional solution at $Pe = 1.4354$ was obtained and the fully developed Nu_T of 7.9635 from the present work is in excellent agreement with the value of 7.964 given in Shah and London [2].

Table 5. Fully developed Nu_T as a function of Pe

Pe	Present solution	Ref. [2]
0.7	8.0363	
1.4	7.9668	
1.4364	7.9635	7.964
3.5	7.8160	
7	7.6838	
10.5	7.6231	
14	7.5926	

The extrapolated values of the fully developed incremental heat transfer number $N_T(\infty)$ at $Pr = 0.7$ are given in Table 6.

For $Pr = 0.7$ and $1 \leqslant Re \leqslant 20$, the following correlation can be used to approximate the data in Table 6 with the error ranging from 0.4% at $Re = 20$ to 3.4% at $Re = 5$:

$$N_T(\infty) = 0.006778 + 0.9756/Re. \quad (14)$$

The dimensionless thermal entrance lengths $L_{th,T}^*$ defined by $Nu_{x,T}(L_{th,T}^*) = 1.05Nu_T$, are given in Table 7.

Equation (15) correlates these values with the deviation ranging from 0.3% at $Re = 20$ to 3.7% at $Re = 2$

$$L_{th,T}^* = 0.0003545 + 0.2643/Re. \quad (15)$$

5. CONSTANT WALL HEAT FLUX RESULTS

In the case of constant wall heat flux, the axial heat conduction within the fluid is constant and therefore does not affect the Nusselt number. The fully developed Nusselt number in this case is 8.2353 and is independent of the Péclet number. Table 8 presents the extrapolated fully developed incremental heat transfer number $N_H(\infty)$ obtained in the present work.

For $Pr = 0.7$ and $1 \leqslant Re \leqslant 20$, the following correlation is provided to approximate the values in Table 8 with the error ranging from 0% at $Re = 5$ to 1.4% at $Re = 20$:

$$N_H(\infty) = 0.04423 + 0.6134/Re. \quad (16)$$

The dimensionless thermal entrance length $L_{th,H}^*$ presented in Table 9 can be calculated from the following equation with the deviation ranging from

Table 6. Fully developed incremental heat transfer number $N_f(\infty)$ at $Pr = 0.7$

Re	1	2	5	10	15	20
$N_f(\infty)$	0.9781	0.5046	0.2002	0.1009	0.07038	0.05638

Table 7. Thermal entrance length $L^*_{\text{th},T}$

Re	1	2	5	10	15	20
$L^*_{\text{th},T}$	0.2655	0.1309	0.05278	0.02686	0.01866	0.01405

Table 8. Incremental heat transfer number $N_H(\infty)$ at $Pr = 0.7$

Re	1	2	5	10	15	20
$N_H(\infty)$	0.6568	0.3526	0.1669	0.1067	0.08417	0.07389

Table 9. Thermal entrance length $L^*_{\text{th},H}$

Re	1	2	5	10	15	20
$L^*_{\text{th},H}$	0.2635	0.1355	0.05855	0.03380	0.02534	0.02124

0.07% at $Re = 1$ to 1.6% at $Re = 20$:

$$L^*_{\text{th},H} = 0.008146 + 0.2552/Re. \quad (17)$$

6. CONCLUSIONS

An analysis has been presented for the flow and heat transfer in the entrance region of parallel horizontal plates at low Reynolds numbers. The Navier–Stokes and energy equations have been solved more accurately than previously with the use of the Richardson extrapolation to zero mesh size. Correlating equations (12)–(17) give fully developed incremental pressure drop number and incremental heat transfer numbers, as well as thermal entrance lengths, for use in the design of parallel plate heat exchangers. All the quantities presented are found to correlate very well with $1/Re$ for the range of Re considered.

REFERENCES

1. I. L. Maclaine-cross and C. W. Ambrose, Predicted and measured pressure drop in parallel plate rotary regenerators, *J. Fluids Engng* **102**(1), 59–63 (1980).
2. R. K. Shah and A. L. London, *Laminar Flow Forced Convection in Ducts*. Academic Press, New York (1978).
3. T. V. Nguyen and I. L. Maclaine-cross, Incremental pressure drop number in parallel-plate heat exchangers, *J. Fluids Engng* **110**(1), 93–96 (1988).
4. R. K. Shah, Thermal entry length solutions for the circular tube and parallel plates, *Proc. 3rd Natn. Heat Mass Transfer Conf.*, Indian Institute of Technology, Bombay, Vol. I, Paper No. HMT-11-75 (1975).
5. C. I. Hwang and F. T. Fan, Finite difference analysis of forced-convection heat transfer in entrance region of a flat rectangular duct, *Appl. Scient. Res., Section A* **13**, 401–422 (1963).
6. I. L. Maclaine-cross, A theory of combined heat and mass transfer in regenerators, Ph.D. Thesis, Department of Mechanical Engineering, Monash University, Australia (1974).
7. B. P. Leonard, A stable and accurate convective modelling procedure based on quadratic upstream interpolation, *Comp. Meth. Appl. Mech. Engng* **19**, 59–98 (1979).
8. T. V. Nguyen, I. L. Maclaine-cross and G. de Vahl Davis, *Numerical Methods in Heat Transfer* (Edited by R. W. Lewis, K. Morgan and O. C. Zienkiewicz), pp. 349–372. Wiley, New York (1981).
9. R.-Y. Chen, Flow in the entrance region at low Reynolds numbers, *J. Fluids Engng* **95**, 153–158 (1973).

ECOULEMENT EN DEVELOPPEMENT A FAIBLE NOMBRE DE REYNOLDS A L'ENTREE DE PLAQUES PARALLELES EN CASCADE

Résumé—On présente les résultats d'une étude numérique du développement d'un écoulement, à faible nombre de Reynolds, à l'entrée d'une région avec des plaques horizontales en cascade et un écoulement uniforme en amont. Les équations aux différences finies de Navier–Stokes et d'énergie, en tenant compte de la diffusion axiale de quantité de mouvement et de chaleur, sont résolues par les méthodes ADI et QUICK et les résultats sont extrapolés à une dimension nulle de maille par l'extrapolation de Richardson. Les résultats pour l'écoulement isotherme, pour les nombres de perte de pression et du transfert thermique, pour les longueurs d'entrée hydrodynamique et thermique sont présentés pour $Pr = 0,7$ et un nombre de Reynolds entre 1 et 20, pour une température de paroi ou un flux pariétal uniforme. On obtient des formules pratiques précises pour l'effet du nombre de Reynolds sur les différentes caractéristiques.

ENTWICKLUNG EINER EINLAUFSTRÖMUNG ZWISCHEN PARALLELEN PLATTEN BEI KLEINER REYNOLDS-ZAHL

Zusammenfassung—Die Ergebnisse der numerischen Berechnung einer sich bei kleiner Reynolds-Zahl entwickelnden Strömung im Einlaufgebiet einer Anordnung paralleler waagerechter Platten wird dargestellt, und zwar für den Fall einer gleichförmigen Anströmung. Die partiellen Differentialgleichungen für den axialen Transport von Impuls und Wärme werden in Differenzenform überführt und mit Hilfe des ADI- und QUICK-Verfahrens gelöst. Die Ergebnisse werden mit Hilfe des erweiterten Richardson-Verfahrens auf die Gittergröße 0 extrapoliert. Für $Pr = 0{,}7$ und Reynolds-Zahlen zwischen 1 und 20 werden als Ergebnis die folgenden Größen vorgestellt: Resultate für isotherme Strömung, zusätzlicher Druckabfall, Kennzahlen für den Wärmeübergang, hydrodynamische und thermische Einlauflängen. Die Berechnungen erfolgen für konstante Wandtemperatur und konstante Wärmestromdichte an der Wand als Randbedingungen. Zusätzlich werden für praktische Berechnungen Korrelationen für den Einfluß der Reynolds-Zahl auf verschiedene Größen angegeben.

СОВМЕСТНО РАЗВИВАЮЩИЕСЯ ТЕЧЕНИЯ С НИЗКИМИ ЧИСЛАМИ РЕЙНОЛЬДСА ВО ВХОДНОМ УЧАСТКЕ ПАРАЛЛЕЛЬНЫХ ПЛАСТИН

Аннотация—Приводятся результаты численного исследования совместно развивающихся течений при низком числе Рейнольдса во входном участке каскада параллельных горизонтальных пластин при равномерном распределении скоростей вверх по потоку. Конечно-разностные соотношения, входящие в дифференциальные уравнения сохранения энергии в частных производных и описывающие аксиальную диффузию импульса и тепла, решаются методами ADI и QUICK, и полученные результаты экстраполируются на размер ячейки сетки, равный нулю, с применением расширенной экстраполяции Ричардсона. Представлены результаты расчета изотермического течения, перепада добавочного давления и чисел теплопереноса, а также длины гидродинамического и теплового начальных участков при $Pr = 0{,}7$ и числе Рейнольдса, изменяющемся от 1 до 20, и при граничных условиях с постоянной температурой стенки и постоянным тепловым потоком. Получены точные инженерные соотношения для учета влияния Re на различные параметры.